



# Effects of Confinement on Opposed-Flow Flame Spread over Cellulose and Polymeric Solids in Microgravity

Ankit Sharma<sup>1</sup> · Yanjun Li<sup>1</sup> · Ya-Ting T. Liao<sup>1</sup> · Paul V. Ferkul<sup>2,3</sup> · Michael C. Johnston<sup>3</sup> · Charles Bunnell<sup>4</sup>

Received: 25 January 2024 / Accepted: 12 March 2024 / Published online: 1 April 2024  
© The Author(s) 2024

## Abstract

Opposed-flow flame spread over solid materials has been investigated in the past few decades owing to its importance in fundamental understanding of fires. These studies provided insights on the behavior of opposed-flow flames in different environmental conditions (e.g., flow speed, oxygen concentration). However, the effect of confinement on opposed-flow flames remains under-explored. It is known that confinement plays a critical role in concurrent-flow flame spread in normal and microgravity conditions. Hence, for a complete understanding it becomes important to understand the effects of confinement for opposed-flow flames. In this study, microgravity experiments are conducted aboard the International Space Station (ISS) to investigate opposed-flow flame spread in different confined conditions. Two materials, cotton-fiberglass blended textile fabric (SIBAL) and 1 mm thick polymethyl methacrylate (PMMA) slab are burned between a pair of parallel flow baffles in a small flow duct. By varying the sample-baffle distance, various levels of confinement are achieved ( $H=1-2$  cm). Three types of baffles, transparent, black, and reflective, are used to create different radiative boundary conditions. The purely forced flow speed is also varied (between 2.6 and 10.5 cm/s) to investigate its interplay with the confinement level. For both sample materials, it is observed that the flame spread rate decreases when the confinement level increases (i.e., when  $H$  decreases). In addition, flame spread rate is shown to have a positive correlation with flow speed, up to an optimal value. The results also indicate that the optimal flow speed for flame spread can decrease in highly confined conditions. Surface radiation on the confinement boundary is shown to play a key role. For SIBAL fabric, stronger flames are observed when using black baffles compared to transparent. For PMMA, reflective baffles yield stronger flames compared to black baffles. When comparing the results to the concurrent-flow case, it is also noticed that opposed-flow flames spread slower and blow off at larger flow speeds but are not as sensitive to the flow speed. This work provides unique long-duration microgravity experimental data that can inform the design of future opposed-flow experiments in microgravity and the development of theory and numerical models.

**Keywords** Opposed-flow flame spread · Microgravity combustion · Confined space · Flame-wall interactions · Confined combustion

## Introduction

Fires in space vehicles and aboard the International Space Station (ISS) can pose a significant risk to the mission, crew, and spacecraft. Hence it is crucial to develop understanding of material flammability in actual spacecraft environments (microgravity). Flame spread is one of the most important characteristics of material flammability as it indicates how fast a flame would travel and potentially ignite nearby materials. Many experiments have been carried out to study the fundamental nature of fire spread over solid combustibles in microgravity conditions using drop towers (Bhattacharjee et al. 2003; Carney et al. 2021; Olson et al. 1989; Olson

✉ Ankit Sharma  
ankit.sharma@case.edu

✉ Ya-Ting T. Liao  
yating.liao@case.edu

<sup>1</sup> Case Western Reserve University, Cleveland  
OH-44106, USA

<sup>2</sup> USRA, NASA Glenn Research Center, Cleveland  
OH-44135, USA

<sup>3</sup> National Aeronautics and Space Administration,  
Cleveland OH-44135, USA

<sup>4</sup> ZIN Technologies, Middleburg Heights OH-44130, USA

and Miller 2009; Vetturini et al. 2020; Zhu et al. 2022), parabolic flights (Consalvi et al. 2021; Feier et al. 2002; Guibaud et al. 2020; Kleinhenz et al. 2008; Konno et al. 2022; Nagachi et al. 2021), space shuttles (Li et al. 2019; Sacksteder et al. 1998), and facilities aboard the ISS (Bhattacharjee et al. 2017; Huang et al. 2019; Li et al. 2021a; Li et al. 2021b). These tests provided insights on the effect of different environmental conditions (e.g., oxygen level, pressure, flow speed) and flow configurations on the flame growth and flame spread rate. Comparisons of concurrent-flow results in different NASA projects such as Burning and Suppression of Solids (BASS) (Zhao et al. 2017) and Safire (Urban et al. 2019) highlighted that flame spread rate is also affected by the confinement level. Even in normal gravity, constrained geometries can enhance (or even hinder depending upon the cavity size) fire spread due to the chimney effect, such as what happened in the London Grenfell Tower Fire accident in 2017 (Sharma and Mishra 2021).

The buoyant flow in a normal-gravity Earth environment establishes a positive feedback loop between the supply of oxygen and the growth of the fire (Comas et al. 2015; Cui et al. 2023; Matsuoka et al. 2018). This buoyancy-induced convection enhances the availability of oxygen, promoting the rapid expansion of the flames, especially in concurrent flow. For opposed flow, however, buoyant flow in some cases may promote blow off extinction (Olson et al. 1989). On the other hand, in microgravity the absence of buoyancy usually means that another oxygen transport method must be provided to enable fire spread. Flames may still be possible simply due to air circulation in the space station or crew vehicle ventilation systems (around 10 to 20 cm/s). However, if the airflow in microgravity is less than around 10 cm/s, the system enters the “oxygen-limited regime,” where the flame weakens and moves away from the solid surface and towards fresh oxygen in the environment. Consequently, the increased flame standoff distance weakens the transfer of heat from the flame to the fuel surface, causing a decrease in the spread rate. For thin cellulose sheets, (Olson et al. 1989) observed that this oxygen-limited behavior is observed when the flow falls below 15 cm/s for a 30% oxygen concentration and below 25 cm/s for a 21% oxygen concentration. Confinement exacerbates the deficiency of oxygen, especially in microgravity, further complicating the flame spread process by exploring the relationship between airflow speed and flame spread, we can gain valuable insights into the dynamics of fire behavior and develop more effective fire safety measures.

Considering these, (Li et al. 2021a) investigated the effect of confinement on concurrent-flow flame spread in microgravity in the “Confined Combustion” ISS project. Here, the BASS hardware (Zhao et al. 2017) was refurbished and modified to allow different levels of flow confinement and

different radiative wall properties. The results demonstrated that at the same confined condition, steady-state flame length and spread rate are proportional to the concurrent flow speed over the tested range. When confinement increases, the flame spread rate and flame length first increase and then decrease. The work stressed that a long test duration is needed to reveal the various stages of flame development, such as accelerating flame spread, steady state, and extinction, under different confinement levels.

Other studies have investigated opposed-flow flame spread (Huang and Gao 2021), with most focusing on flow speed, oxygen concentration, fuel thickness, fuel width, and radiation feedback in actual (Bhattacharjee et al. 2016; Bhattacharjee and Carmignani 2022; Carmignani et al. 2020; Kashiwagi et al. 1996; Olson et al. 2001; Olson 1991; Takahashi et al. 2002; Urban et al. 2019; Wang et al. 2015) or simulated (Hossain et al. 2018, 2020; Olson et al. 2009; Zhang and Yu 2011) microgravity conditions. A few studies have specifically examined the impact of confinement on opposed-flow flame spread. For instance, Nakamura et al. (Konno et al. 2020) conducted numerical simulations to investigate enclosure effects on opposed-flow flame spread and observed that flame spread rate was faster for the enclosed case than the open case. Wang et al. (Wang et al. 2015) conducted experiments using a drop tower to investigate the impact of confinement on the flame spread over thin solid fuels in a low speed opposing flow (5 cm/s). Their results revealed a non-monotonic trend of flame spread rate with respect to the height of the tunnel where the flame spread occurred. However, it is important to note that the tests were conducted at a single flow speed and were limited to a duration of 3.6 s due to the inherent constraints of achieving microgravity conditions on Earth (e.g., the limiting height of the drop tower).

Additional studies examined longer durations by using a simulated microgravity environment in normal gravity (Hossain et al. 2018; Olson et al. 2009). (Olson et al. 2009) developed a Narrow Channel Apparatus (NCA) that physically constrains buoyant convection by using short-height channels. Opposed-flow flame spread experiments were performed at different flow speeds, oxygen concentrations, and channel gap sizes. Good agreement was obtained between the results from the NCA, and corresponding equivalent tests performed at the NASA microgravity drop facilities. (Hossain et al. 2018) further investigated various channel heights and airflow speeds for opposed-flow flame spread over thin fuels using the NCA. It was noted that only limited confinement levels can be studied in NCA since making the gap too narrow yields excessive heat loss to the confining walls and making the gap too large nullifies the simulated microgravity conditions because significant buoyant flow can develop.

Furthermore, as reported by (Li et al. 2021a) in the case of concurrent flow a longer testing duration is needed to reveal the various stages of flame development, such as accelerating flame spread, steady state, and extinction, under different confinement levels. To the best of the authors' knowledge, no other experiments have been conducted that specifically examine the impact of confinement on fire behavior in long-duration opposed-flow microgravity conditions, the objective of the present study. This work focuses on investigating the impact of confinement on flame behavior and spread for long duration microgravity conditions in different opposing airflows. The study also investigates the radiative interactions between the flame and surrounding walls. Our ultimate goal is to gain insights that could be useful in identifying risks in future structural designs and enhancing fire safety codes for space and Earth applications.

## Microgravity Experiments

This work presents additional results from the Confined Combustion ISS project. Specifically, we will present the opposed-flow flame spread data for the cotton-fiberglass composite fabric fuel (also called "SIBAL fabric") and PMMA. Results of the concurrent-flow portion of the project have been published in separate papers (Li et al. 2021b; Li et al. 2021a).

## Experiment Facility

The experimental apparatus is shown in Fig. 1. It is identical to that reported in (Li et al. 2021a) except for the fuel

ignited on the downstream trailing edge (to initiate the opposed-flow flame spread), and thus will be described here only briefly. Cotton-fiberglass composite fabric fuel samples and 1-mm-thick PMMA (the same as used in (Li et al. 2021a; Olson et al. 2021; Zhao et al. 2017) are burned in an opposed flow in the BASS flow duct located in the Microgravity Science Glovebox (MSG) aboard the ISS. The flow duct is 20 cm long and has a square cross-Sect. 7.6 cm by 7.6 cm. A fan provides a variable forced convective flow up to 55 cm/s. (Flow speeds reported here are the average value at a given cross section.) The MSG is equipped with an O<sub>2</sub> sensor (Quantek model 201) that has an accuracy  $\pm 2\%$  of reading. This sensor is installed to monitor the oxygen consumption in the MSG during each test. In addition, the environmental oxygen sensor data is also collected from the ISS. In this study, all experiments are conducted at ISS ambient conditions i.e., at 1.0 atm and  $\sim 22\%$  oxygen mole fraction (with daily oxygen variation between 21.3% and 22.9%). The burning events are recorded by a video camera through the top window of the flow duct. The video recordings have a spatial resolution of 12.5 pixels/mm (equivalent to 0.08 mm/pixel) and a frame rate of 24 frames per second. The camera is configured to automatically adjust for white balance, exposure, and digital gain.

## Sample-Baffle Assembly and test Matrix

The study involves evaluating the SIBAL fabric (75% cotton, 25% fiberglass, area density: 18 mg/cm<sup>2</sup>, 0.33 mm thick) and PMMA materials, which were previously assessed in BASS (Olson et al. 2021; Zhao et al. 2017) and in the concurrent-flow tests in Confined Combustion. Both samples

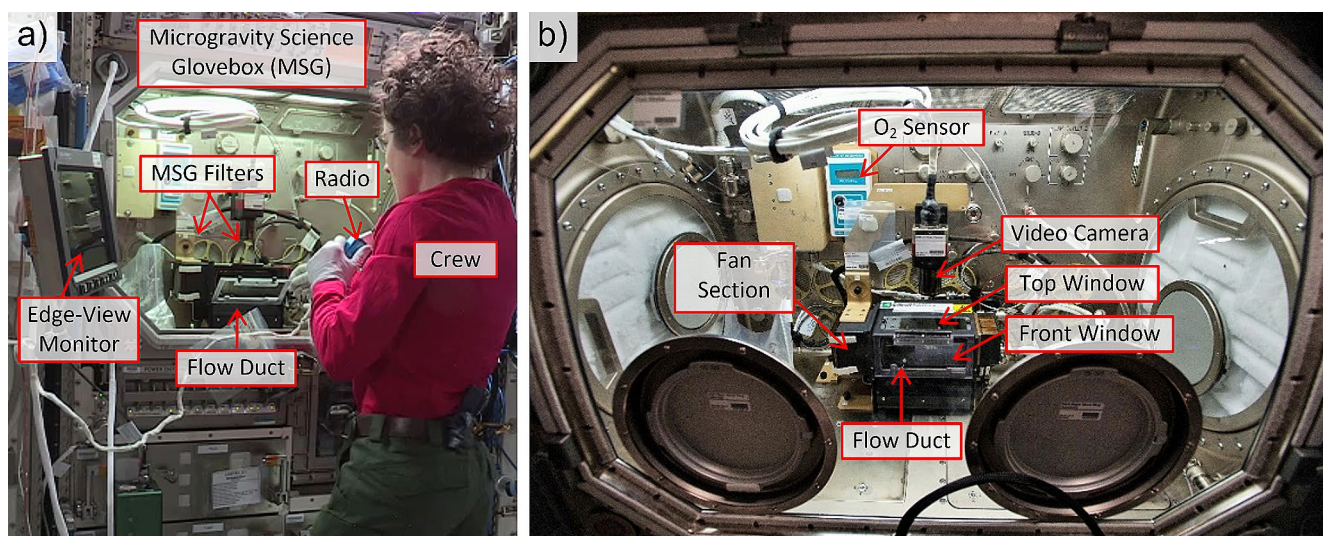


**Fig. 1** Experimental setup of the BASS hardware in the Microgravity Science Glovebox aboard the International Space Station. (a) ISS crew member performing a test with real-time communication with the sci-

ence team located at the NASA Glenn Research Center ISS Payload Operations Center (GIPOC). (b) Close-up view of the experimental setup (Li et al. 2021a)

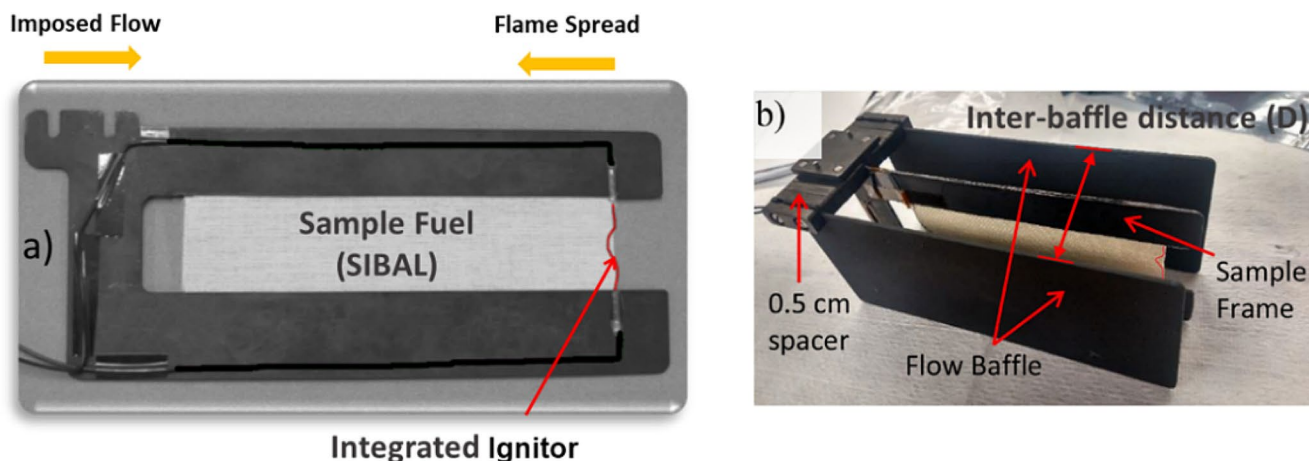


**Fig. 2** Sample setup. (a) Sample holder with fuel and igniter mounted. (b) Assembly of baffle/sample system showing sample, sample frame, and two parallel black baffles

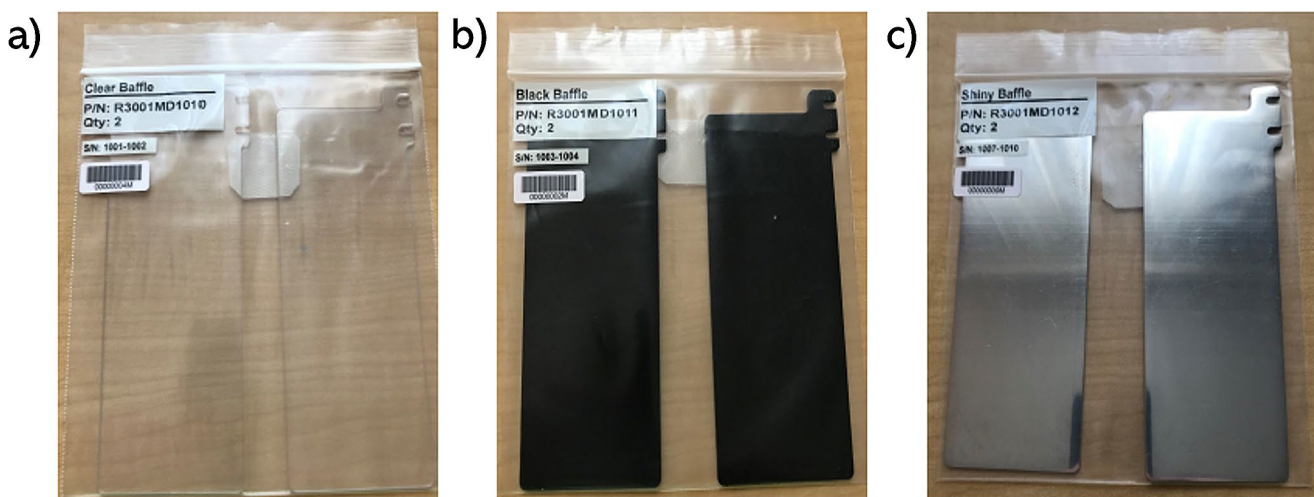


**Fig. 3** Types of flow baffles. (a) Transparent polycarbonate. (b) Anodized black aluminum. (c) Reflective aluminum

are considered thermally thin in the experiments. The sample is held between two thin, stainless steel, black-oxide-treated sample frames that are 13.8 cm long and 6.1 cm wide (Fig. 2a). The exposed area of the sample is 10 cm long and 2.2 cm wide (Fig. 2a). A 29-AWG Kanthal hotwire of resistance  $\sim 1 \Omega$  located at the downstream edge of the sample is used to ignite the samples. After ignition, the samples are allowed to burn in the opposed-flow configuration. A newly developed baffle/sample system enables the creation of different confinement conditions inside the flow duct (Fig. 2b). The sample frame is installed at the center position of a mounting system, with two parallel flat baffles on each side of the sample (Fig. 2b). The dimensions of the baffles are the same as those of the exterior measurements of the black stainless steel sample holder. The mounting system comprises a series of 5 mm spacers. By adjusting the number of spacers between the baffles and the sample, various levels of flame confinement can be achieved.

Three types of baffles, namely transparent polycarbonate, black anodized aluminum, and polished (reflective) aluminum are used to study the impact of radiative boundary conditions (Fig. 3). The surface properties and other details of these baffles can be found in (Li et al. 2021a). To facilitate the attachment of the baffle/sample assembly to the BASS flow duct, the top window of the flow duct is retrofitted, and the assembly is magnetically integrated with the top window mount. This new design ensures that the sample is centered in the middle of the flow duct.

Arrangement of baffles and sample is sketched in Fig. 4. The flame burns on both sides of the SIBAL fabric while for the PMMA, the flame is only allowed on one side. Note that the weaker, single-sided flame is preferred in the PMMA tests to protect the baffles from thermal damage as observed in the concurrent tests (Li et al. 2021b). The single-sided flame configuration is achieved by installing a quenching baffle, 5 mm away from the back side of the sample. The

**Fig. 4** Sample/baffle configuration for (a) SIBAL (b) PMMA (H: sample-baffle distance; 2 H = D: inter-baffle distance for SIBAL)

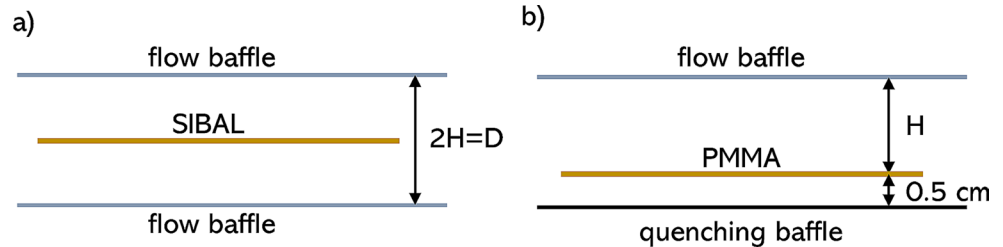


**Table 1** Test matrix for SIBAL and PMMA

Sample	Burning scenario	Baffle type (boundary wall condition)	Sample-baffle distance (H in cm)	Opposed-flow speed <sup>a</sup> (cm/s)
SIBAL	Double sided	Anodized black aluminum	1.5	10.3 <sup>b</sup> → 7.3 → 6.1 <sup>c</sup>
		Transparent polycarbonate	2.0	10.3 <sup>b</sup> → 7.3 <sup>c</sup>
		Transparent polycarbonate	1.0	10.5 <sup>b</sup> → 8.8 → 7.4 <sup>c</sup>
		Transparent polycarbonate	1.5	10.3 <sup>b</sup> → 7.3 → 6.1 <sup>c</sup>
PMMA	Single sided	Anodized black aluminum	1.5	7.31 <sup>b</sup> →10.3→7.3→6→4.7→3.2→10.3 <sup>c</sup>
		Reflective aluminum	1.5	7.31 <sup>b</sup> →6→4.7→3.2 →2.6 <sup>d</sup>

<sup>a</sup> Crew manually adjusts flow rate with a dial between opposed flow speed setpoints

<sup>b</sup> Initial flow speed for ignition

<sup>c</sup> Flame sustained and consumed the sample at this flow speed (i.e., flame reached end of sample)

<sup>d</sup> Flame quenched within 10 s at this flow speed

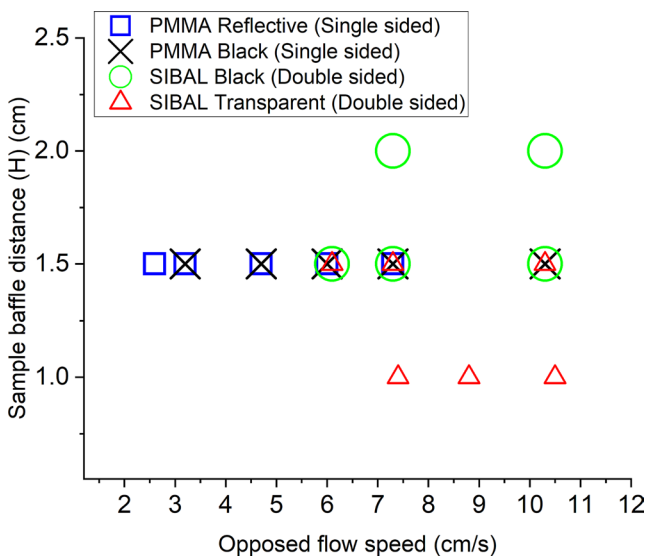


**Fig. 5** Test matrix for SIBAL and PMMA samples in opposed flow confined combustion

flame cannot be established in this narrow gap because there is minimal air flow and excessive conductive heat loss for any flame that might try to become established there. For the thin SIBAL samples, flame residence time over the sample is short and heat transfer to flow baffles is not as significant, so a two-sided flame is permitted.

The test matrix for SIBAL and PMMA is shown in Table 1; Fig. 5. Key variables in the study are flow speed (ranging from 2.6 to 10.5 cm/s) and confinement level (i.e., sample-baffle distance H, at 1, 1.5, and 2 cm depending upon

the sample). Preflight flow calibration performed at various sample-baffle distances and at three different streamwise locations (near the entrance, at the center, and near the exit of the duct) is discussed in detail in our previous work (Li et al. 2021a). In this study, flow speed is decreased in steps as the flame spreads over the sample. After each flow reduction, the flow speed is maintained for a certain period (~20 s for SIBAL and ~200 s for PMMA) to allow the flame to reach steady state at the new flow condition. It is noted that flames in the opposed-flow configuration exhibit rapid response to changes in flow conditions. This is because the preheating of the fuel and hence the flame spread rate rely mainly on radiation and thermal diffusion in a small region surrounding the upstream flame base stabilization zone. This characteristic of opposed-flow flames is used to observe and analyze the flame spread behavior as a function of flow speed by conducting a series of incremental flow adjustments in a single test. This procedure is similar to that used in the previous BASS tests and allows multiple flow speeds to be examined in one burn (Zhao et al. 2017).

## Results and Discussions

### Transient Flame Development Process

The process of flame development resulting in steady, spreading flames at each flow step for SIBAL is illustrated in Fig. 6. In this case, two black baffles are used with a 1.5 cm

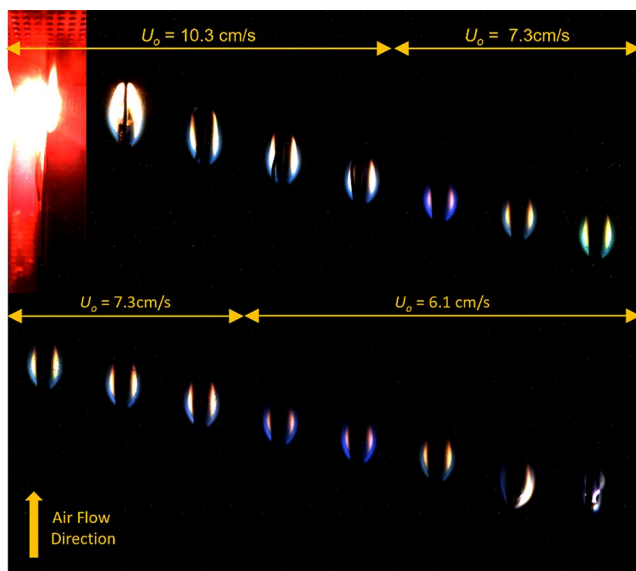


**Fig. 6** Opposed-flow flame spread over SIBAL fabric sample. Confined conditions: black anodized aluminum baffles with 1.5 cm sample-baffle distance ( $H$ ). Ignition is at upper left, and images are 5 s apart, left to right, top row to bottom row

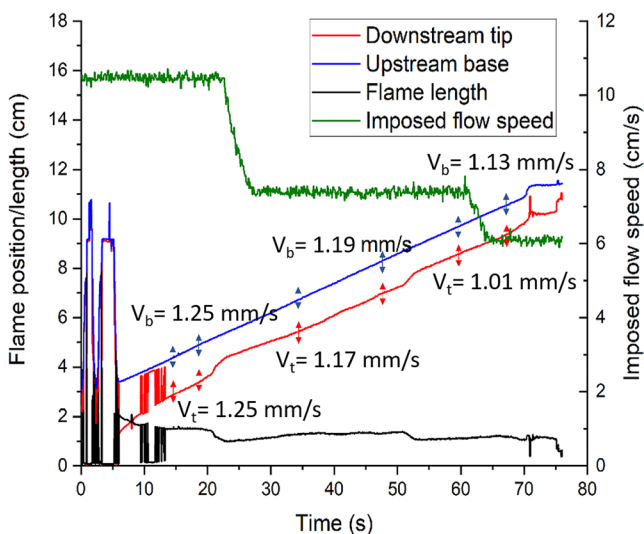


**Fig. 7** Flame location versus time for opposed-flow flame spread over SIBAL fabric sample with flow speeds shown in green. Confined conditions: black anodized aluminum baffles with 1.5 cm sample-baffle distance ( $H$ ).  $x=0$  is defined at the downstream trailing edge of the sample

sample-baffle distance ( $H$ , see Fig. 4a). The opposed flow is decreased from 10.3 to 6.1 cm/s in two steps. Following activation of the hotwire ignitor, the solid fuel is heated and pyrolyzed and a gaseous flame initiates at the downstream trailing edge of the sample and propagates against the flow until the sample is completely burned. Decreasing the flow speed results in a bluish color of the flame, indicating reduced formation of soot and possible lower flame temperature, along with a decrease in flame length and spread rate.

The flame position, spread rate, and imposed flow speed are depicted in Fig. 7. The video frames are processed using a custom-built code using MATLAB Image Analysis Toolbox, which converts the images to binary format, detects the flame boundary, and monitors the flame position over time. The specifics of the code and the methodology used to track the flame location are described in previous research (Li et al. 2021a).

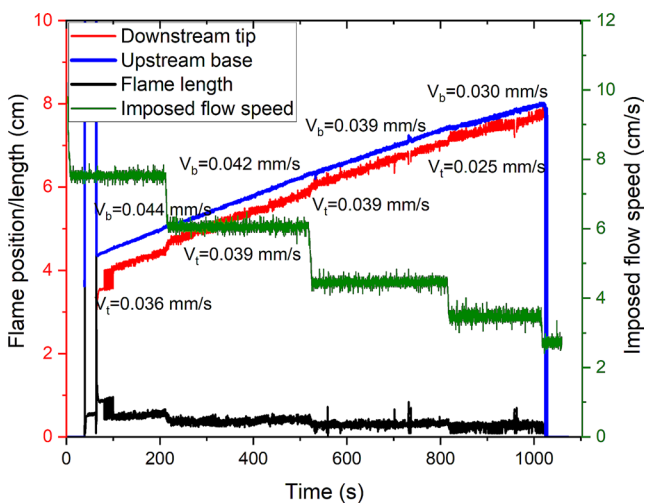
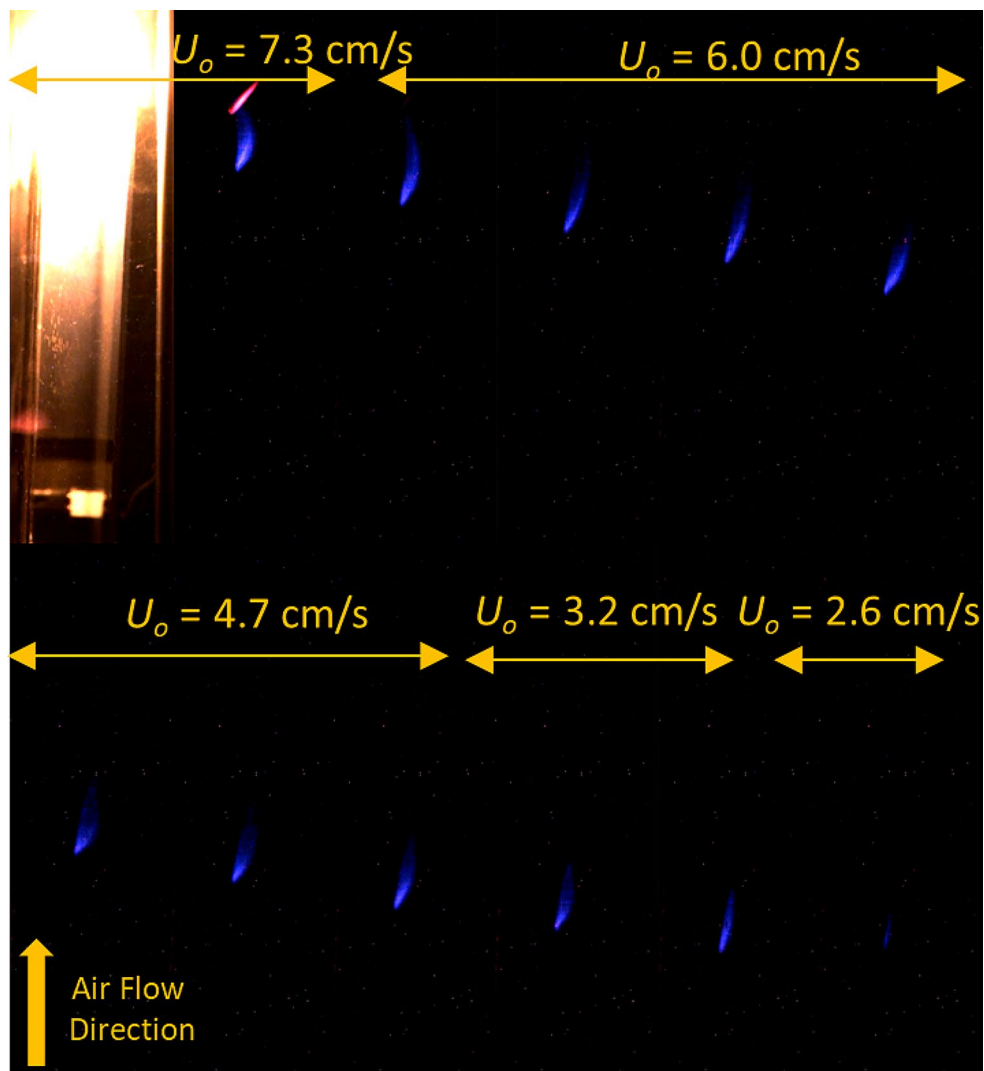
At the beginning of the video recording, the igniter emits bright light that saturates the camera, making it difficult to accurately identify the flame's location. However, as soon as the igniter is turned off, the flame reaches a steady spread rate and length at the three tested flow rates (10.3, 7.3, and 6.1 cm/s, respectively). The steady flame spread rates ( $V_t$  and  $V_b$  for downstream flame tip and upstream base, respectively) are deduced in time periods bounded by small vertical arrows in Fig. 7. For each flow rate tested, a linear least-squares curve fitting method is used to determine the flame spread rate, and the average visible flame length is calculated for each steady spread stage. Similar observations of steady flame length and spread rate are made in other SIBAL tests as well. In general, the spread rate and flame length decreased with the imposed flow speed and the sample-baffle distance. This will be discussed further in the next section.

Figure 8 depicts a typical flame development process resulting in steady, spreading one-sided flames at each flow step for PMMA. Two reflective baffles with 1.5 cm sample-baffle distance ( $H$ ) (see Fig. 4b) are used in this case, and the opposed-flow speed is gradually decreased from 7.3 to 2.6 cm/s in four steps. Following activation of the ignitor, a gaseous flame emerges at the downstream trailing edge of the sample and propagates against the flow until the sample is completely burned. The flame appears mostly blue right from the start, indicating minimal soot formation. Compared to the SIBAL fabrics, the PMMA samples have smaller flame lengths and spread rates. Flame position, spread rates, flame length, and flow speed are shown in Fig. 9. Similar to the SIBAL fabric samples, steady-state flame spread is observed for PMMA samples, both for reflective and black baffles.

### Effects of Confinement and flow Speed

Figure 10 illustrates the flame profiles for SIBAL fabric at different sample-baffle distances, all at the same opposed-flow speed of 7.3 cm/s. As the confinement increases (i.e.,  $H$  decreases from 2.0 cm to 1.5 cm for black baffles and from  $H=1.5$  cm to 1.0 cm for transparent baffles), the flame length reduces due to oxygen starvation (Li and Liao 2022; Olson 1991; Olson et al. 1989) and heat loss to the baffles (Li et al. 2021a; Li and Liao 2022). This is further discussed

**Fig. 8** Opposed-flow flame spread over PMMA sample. Confined conditions: Reflective aluminum baffles with sample-baffle distance  $H = 1.5$  cm. Ignition is at upper left, and images are 50 s apart, left to right, top row to bottom row



**Fig. 9** Opposed-flow flame location versus time for PMMA sample with flow speeds shown in green. Confined conditions: Reflective aluminum baffles with  $H = 1.5$  cm (sample-baffle distance).  $x = 0$  is defined at the downstream trailing edge of the sample

in the next section on the effect of radiation feedback. It is worth noting that when the flame is small and dim at the smallest baffle distances (e.g.,  $H = 1.0$  cm), the camera struggles with white balance, leading to videos with unrealistic flame colors (as seen in Fig. 10d).

The flame spread rates at different baffle distances are summarized and compared in Fig. 11. When flow speeds are held constant (tested flow speeds are marked next to data points on the plot), the rate of flame spread decreases as the confinement increases. As the distance between sample and baffles ( $H$ ) decreases, two factors come into play: oxygen depletion (Li and Liao 2022; Olson 1991; Olson et al. 1989) and increased net heat loss to the baffles (Li et al. 2021a; Li and Liao 2022). Comparing black anodized aluminum baffles to polycarbonate transparent baffles, the former is anticipated to have higher conductive heat loss and lower spread rates due to their significantly larger thermal conductivity (200 vs. 0.2 W/m/K) and volumetric heat capacity ( $\rho C_p \sim 2.46$  vs. 1.44 J/cm<sup>3</sup>/K). However, contrary

**Fig. 10** Comparisons of opposed-flow flame profiles in different confined conditions at a flow speed of 7.3 cm/s for SIBAL (H is sample-baffle distance)

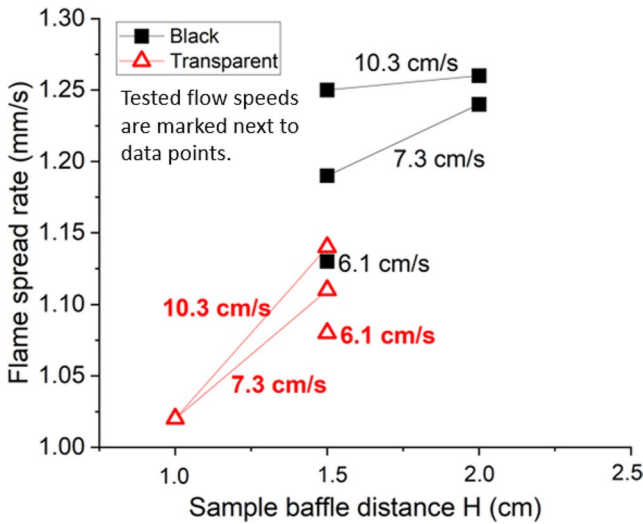
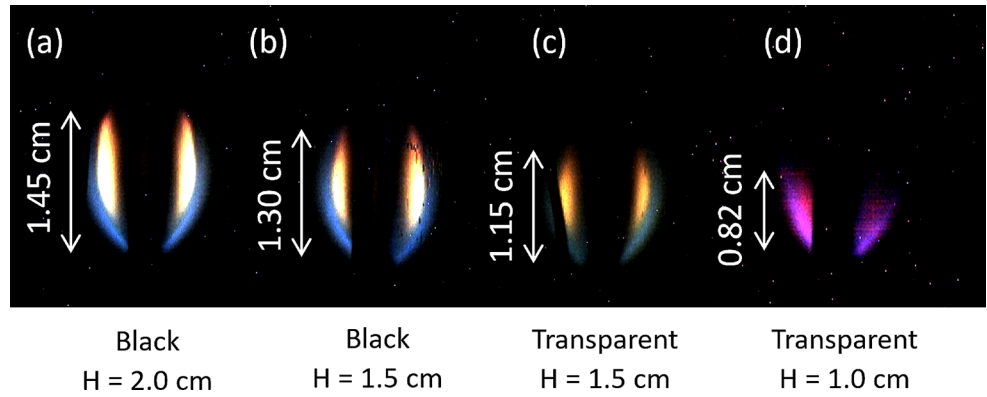


**Fig. 11** Flame spread rates ( $V_b$ ) at different inter-baffle distances (H) for the opposed-flow configuration over SIBAL fabric with black and transparent baffles. Numbers marked next to the data points are the tested flow speeds

to expectations, black anodized aluminum baffles exhibit higher spread rates. This unexpected result is attributed to the relatively higher radiation emission from black baffles compared to transparent ones. Consequently, due to thermal radiation, the net heat loss in black baffles is reduced, leading to higher spread rates (to be discussed further in Sect. 3.3). In Fig. 10, the flame standoff distance (i.e., the maximum distance from the flame to the sample surface) was observed to be ~6 mm in all cases (it decreased slightly when the confinement increased). For the black baffles, if the sample-baffle distance is reduced further (e.g., to  $H \leq 1$  cm) and the flame is in the immediate proximity to the baffles, conductive heat loss from the baffles may become dominant, resulting in higher net heat loss and lower spread rates compared to the transparent baffles (due to the higher conductivity and the higher heat capacity), as observed in the concurrent cases (Fig. 12). However, for the opposed cases, this needs to be confirmed with more experiments as black baffles in the present study were not tested for distances

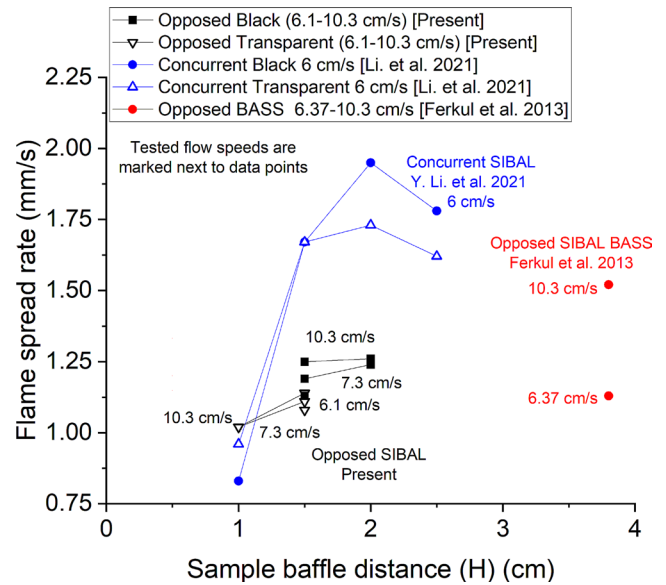


**Fig. 12** Comparison of flame spread rate ( $V_b$ ) at different inter-baffle distance in opposed-flow (present and literature (Ferkul et al. 2013) and concurrent-flow (literature (Li et al. 2021a) experiments for SIBAL. Numbers marked next to the data points are the tested flow speeds

lower than  $H = 1.5$  cm. Furthermore, at such proximity, the flow viscosity will also significantly reduce the local flow near the sample surface, hindering the flame growth process for much weaker opposed-flow flames.

Figure 12 compares the opposed-flow SIBAL results obtained in this work with previous concurrent flow results in Confined Combustion (2.2 cm wide sample) (Li et al. 2021a) and opposed flow results in BASS (2 cm wide sample) (Ferkul et al. 2013). At sample baffle distance  $H = 1.5$  and 2 cm, the opposed-flow flame spread rates are ~25–36% lower than the concurrent-flow flame spread rates obtained from previous studies (Li et al. 2021a). At the minimum tested baffle distance  $H = 1.0$  cm, with slightly higher flow speeds, the opposed-flow flame spread rates are slightly larger than for concurrent-flow flames. Also, opposed-flow flame spread is not as sensitive to the baffle



distance compared to the concurrent-flow case, with a maximum decrease of  $\sim 5\%$  (for the opposed-flow, transparent baffle case) compared to 50% for the concurrent-flow (black baffle case) when  $H$  changes from 1.5 to 1 cm. Furthermore, in previous concurrent-flow tests, an optimal inter-baffle distance is observed at  $H=2.0$  cm where the spread rate is maximum. However, an optimal distance is not noticed in the present opposed-flow data. This can be due to the limited number of data points. It is also possible that the effects of flow acceleration due to confinement are not as significant for opposed-flow flame spread. For opposed-flow flames, the flow acceleration mainly occurs downstream of the pyrolysis zone in the burnout region. For current-flow flames, the flow acceleration occurs in both pyrolysis and preheat regions, directly resulting in enhanced heat transfer from the flame to the virgin solid fuels. In addition, the opposed-flow flames are generally smaller and hence cause less thermal expansion compared to concurrent-flames.

When comparing the present results with previous opposed-flow tests at lower and higher confinement levels (i.e., sample baffle distance  $H=0.5, 0.9, 3.8$  cm) in Fig. 12, it appears that the opposed-flow spread rate for SIBAL follows a monotonically decreasing trend with increase in confinement levels (i.e., from  $H=3.8$  to 1 cm) due to oxygen starvation and conductive heat loss to the baffles. However, this is different from the non-monotonic trend of flame spread rate with confinement (5 to 1.5 cm) observed in a previous study where a 0.062-mm-thick laboratory wipe was burned at a fixed opposed-flow speed of 5 cm/s in a 3.6 s drop tower (Wang et al. 2015). These differences can be attributed to many factors including different fuel samples, properties, experimental setup, conditions, and duration.

Figure 13 compares the opposed-flow flame spread rate at different flow speeds. When the confinement level is constant, the flame spread rate increases with the increase in flow speed, although only slightly. As flow is increased, the viscous boundary layer becomes thinner and heat flux to the fuel surface increases. There may also be reduced flame radiation percentage loss (Takahashi et al. 2015) and enhanced mixing of fuel and oxidizer, both of which result in increase of the flame spread rate. This agrees with previous research as shown in Fig. 14 (Kleinhenz et al. 2008; Olson et al. 1989) where opposed-flow flame spread rate increases with ambient flow to a maximum when the flow speed is around 20 cm/s. Further, in these previous studies, it was also noted that the opposed-flow spread rate decreases at higher flow speeds due to enhanced cooling effects and a shorter residence time for the gas phase reaction (i.e., the Damkohler number effect), finally leading to blow-off extinction at higher flow speeds. In this study, the maximum flow speed tested is  $\sim 10.5$  cm/s, lower than the optimal flow speed

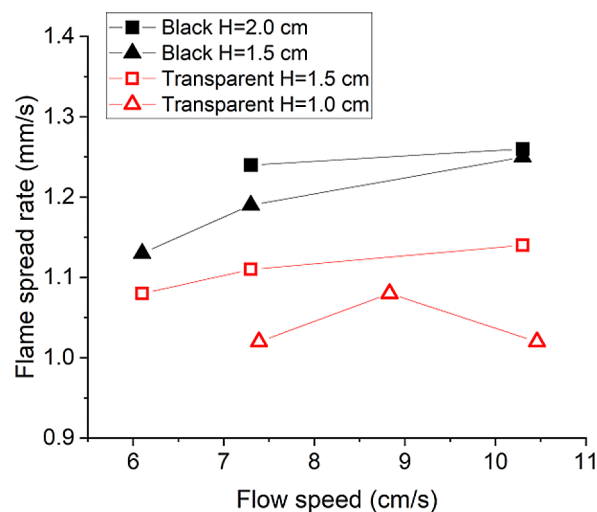


Fig. 13 Flame spread rate at different flow speeds for the opposed-flow configuration over SIBAL fabric with black and transparent baffles

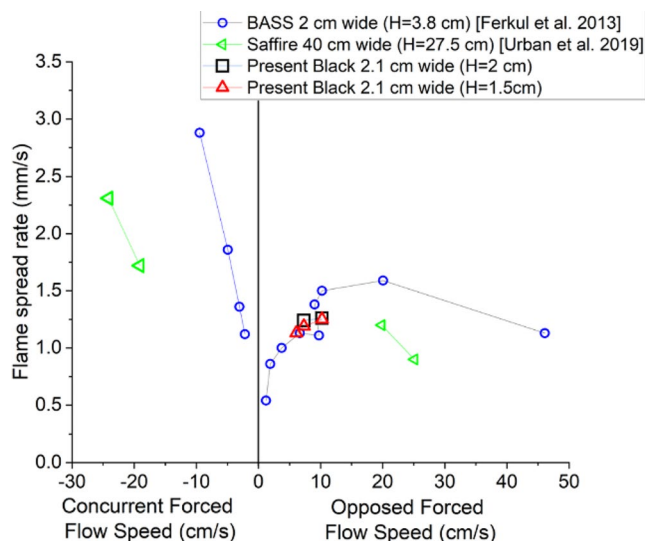


Fig. 14 Flame spread rate for SIBAL fabric at different flow speeds in previous opposed-flow and concurrent-flow experiments (Ferkul et al. 2013) (Urban et al. 2019) with black baffles in present opposed forced flow work

obtained in the previous studies (i.e., 10–15 cm/s) (Olson et al. 1989) and a decrease in opposed-flow spread rate with increase in flow speed is not observed except for the case with the smallest sample-baffle distance at  $H=1$  cm. For this case, the optimal flow speed is observed at  $\sim 8.8$  cm/s (Fig. 13). At such a high confinement level, heat loss to the baffles and reduction of oxygen transport to the combustion zone hinder the gas-phase combustion, requiring a longer flow residence time. As a result, the optimal flow speed and the blow-off limit are expected to be smaller. This shows that confinement plays a significant role and can change the dominant physical processes in fires. It is also clear from Fig. 14 that over the tested flow range, opposed-flow flame

spread is not as sensitive to the variation in the flow speed compared to concurrent flow in previous studies.

Similarly, Fig. 15 compares the flame spread rates for PMMA with reflective and black baffles at 1.5 cm sample-baffle distance. Spread rates for both baffles decrease with the flow speed with higher spread rates for reflective baffles as discussed in the next section. For the reflective baffle case, the sample was not consumed fully, and flame quenched within 10 s after the flow speed was reduced to 2.6 cm/s. For the black baffle case, the sample was fully consumed when the flow speed was reduced to 4.7 cm/s and the low-speed quenching limit was not reached.

Comparisons are also drawn for PMMA in opposed (present and literature (Olson et al. 2021) and concurrent (Confined Combustion data previously reported in (Li et al. 2021b)) flows in Fig. 15. Similar to SIBAL samples, concurrent spread rates are observed to be higher compared to opposed flow spread rates at the same baffle distance and flow speed for PMMA samples. This is because in a concurrent flow, the flame extends downstream and covers the pyrolysis and preheat regions of the solid fuel. In an opposed flow, the flame covers the burned region of the solid fuel and the thermal diffusion occurs against the flow in a small region near the upstream flame base. Therefore, the heat transfer between the flame and the solid fuel is more effective in concurrent than in opposed flows. For the same reason, the no-spread quenching limit occurs at a higher flow speed in the opposed-flow test (2.6 cm/s for reflective baffle) compared to the concurrent-flow test (2.0 cm/s for black baffles (Li et al. 2021b)) at the same confined level ( $H=1.5$  cm). Note that in both concurrent and opposed flow tests, the no-spread limits were determined at the flow speeds for which the flame could not be sustained for more than 10 s.

### Effect of Radiation Feedback

Referring back to Fig. 10b and c for SIBAL, it is observed that when the baffle distance is the same (i.e.,  $H=1.5$  cm), the flame appears longer with black baffles compared to transparent. During the combustion process, some of the heat is lost to the surroundings due to radiation. The baffles absorbed some of the radiation from the flame ( $\sim\alpha\dot{q}_f''$ ), and provided heat feedback to the flame through surface radiation emission ( $\sim\epsilon\sigma T_s^4$ ). With higher absorptivity ( $\alpha$ ) and emissivity ( $\epsilon$ ), the black baffles were expected to absorb a higher fraction of radiation and re-emit it to the sample and the gaseous flame, leading to a longer flame. Conversely, a higher proportion of radiation passes through the transparent baffles and is lost to the ambient, resulting in less heat feedback to the fuel, a lower flame temperature, and a lower flame spread rate (Fig. 11). Similar behavior is seen when

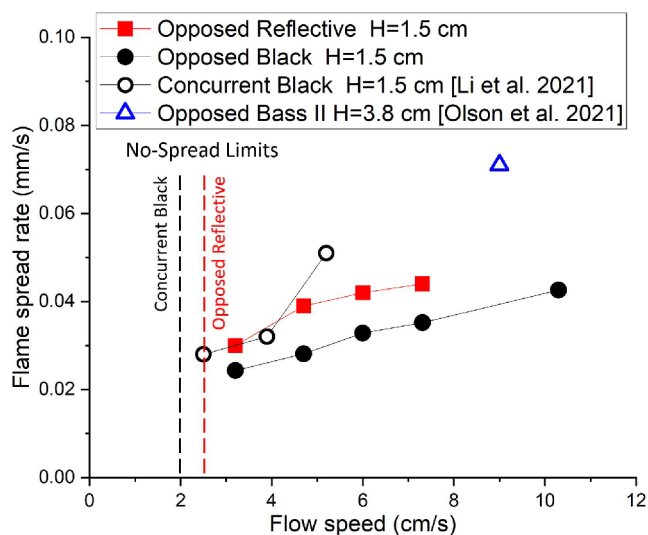


**Fig. 15** Comparison of PMMA flame spread rate at different flow speeds and inter-baffle distances in opposed-flow (present and literature) and concurrent-flow (literature) experiments. No-spread limits were determined at the flow speeds for which the flame was not sustained for more than 10 s

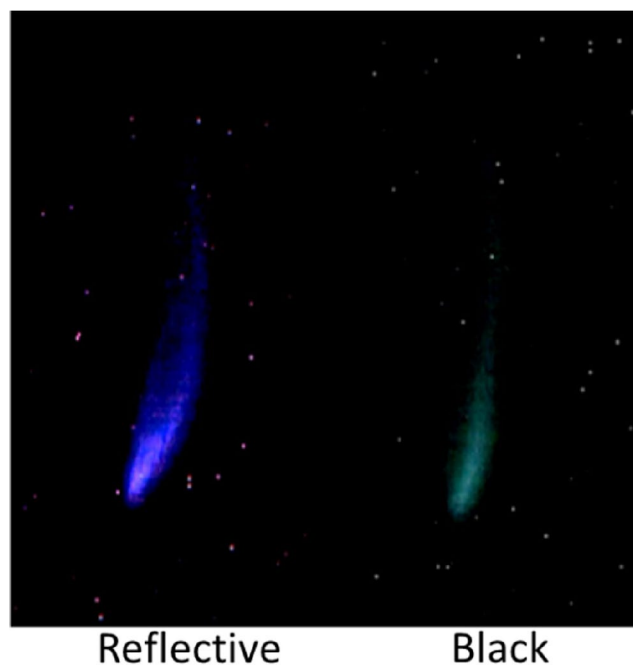


**Fig. 16** Comparison of opposed-flow flame profiles over PMMA in different boundary wall conditions (i.e., reflective, and black baffles) at sample baffle distance  $H=1.5$  cm and flow speed 6.0 cm/s

comparing flame profiles for PMMA in Fig. 16. Longer flames and faster spread rate are observed for the reflective baffles due to enhanced heat feedback to the solid fuel compared to black baffles.

## Concluding Remarks

In the present study, opposed-flow flame spread over thin cotton-fiberglass blend fabrics (SIBAL) and 1-mm-thick PMMA is investigated in a small flow duct aboard the ISS. The opposed flow varies from 2.6 to 10.5 cm/s. Different confinement levels are achieved by placing flow baffles next to the burning sample at different distances ( $H=1-2$  cm). Three different baffle materials, black anodized aluminum, reflective aluminum, and transparent polycarbonate are used to simulate different radiative boundary conditions. Results obtained are compared with previous opposed- and concurrent-flow tests in different confinements. Key findings are as follows.

1. Opposed-flow flame spread rate has been shown to be positively correlated to the ambient flow speed (up to an optimal flow rate). This remains true in this study when the burning is subjected to various levels of confinement. The correlation is stronger for the 1-mm thick PMMA samples than for the thin SIBAL samples. For SIBAL samples at confinement level  $H=1-2$  cm, flame spread rate increases by  $\sim 11\%$  when flow speed increases by  $\sim 70\%$ . For PMMA samples at  $H=1.5$  cm, flame spread rate increases by  $40\%$  when flow speed increases by  $\sim 87\%$ .
2. Confinement introduces heat loss to the surrounding walls (i.e., baffles in this study) and restricts oxygen supply to the combustion zone. As a result, flame spread rate is observed to generally decrease as the confinement level increases. These effects also reduce the gas-phase reaction rate, increase the required flow residence time, and decrease the optimal flow speed. The optimal flow speed for flame spread is found to be around 8.8 cm/s at  $H=1$  cm, lower than the previously reported 15 cm/s for the same sample burning in a taller flow duct (BASS flow duct,  $H=3.8$  cm).
3. The radiation boundary condition in a confined space is shown to play a significant role. For SIBAL samples, at the same confinement level, the black baffles result in a stronger flame with a higher spread rate (12% higher) and a longer flame length compared to the transparent baffles. For PMMA samples, the flame spread rates can be  $\sim 40\%$  higher with reflective baffles compared to black baffles at same confined conditions.
4. Compared to concurrent-flow flame spread, opposed-flow flame spread is less sensitive to the ambient flow speed and the confinement level (over the tested range in this study). In addition, the opposed-flow flame spread rate is generally slower (by  $\sim 25-36\%$  for SIBAL samples) and the low-speed quenching limit is larger (2.6 cm/s vs. 2.0 cm/s for PMMA samples at

$H=1.5$  cm) compared to concurrent-flow flame spread at the same conditions.

5. The opposed-flow SIBAL data from present and previous experiments (BASS) suggested a monotonic decrease of flame spread rate when flow confinement level increases. This is different from the non-monotonic trend observed in a previous microgravity experiment with a short test duration (3.6 s) and confinement level 1.5–5 cm at ambient flow speed of 5 cm/s and may be due to the inherent differences in the fuel sample and experimental setup.

The present work provides unique long-duration microgravity data for understanding the effects of confinement in the opposed-flow flame spread configuration. The time-resolved data can also be used to assess and validate existing and future fire models and theories. However, additional experiments are required to investigate the burning of solids and flame propagation in different confinement conditions. More data points and a comprehensive investigation are needed to achieve a complete understanding of the fire dynamics associated with this burning process. In addition, investigations on how one burning sample ignites the next, the criterion for such ignition to occur, and the interaction of two (or more) burning samples in opposed-flow configurations in different confined conditions also need to be investigated to mitigate fire risk in future space missions.

**Acknowledgements** This research is co-sponsored by the National Science Foundation (NSF) and Center for the Advancement of Science in Space (CASIS) under grant number CBET-1740478. Operations support, payload modifications for Confined Combustion, and the design and manufacturing of the BASS modifications were performed by ZIN Technologies. The original wind tunnel adapted from Enclosed Laminar Flames (ELF) was designed and built by NASA Glenn Research Center. The science team received tremendous support during operations from NASA Glenn Research Center, Marshall Spaceflight Center, and ZIN Technologies. We especially appreciate the support from Emily Griffin, Steve Lawn, Russell Valentine, Beth Curtis, Chris Rogers, Wendell Booth, Michael Hall, and the Microgravity Science Glovebox team. We would also like to express our immense appreciation to our lab partners in space, ISS crew members Christina Koch, Jessica Meir, Andrew Morgan, Luca Parmitano, Shannon Walker, and Michael Hopkins for supporting and conducting the microgravity experiments aboard the ISS.

**Author Contributions** A. S. performed research, analyzed data, and prepared the manuscript. Y. L. performed research and analyzed data. Y.-T. T. L. advised the research, supported the ISS operations, and revised the manuscript. P. V. F. and M. C. J. provided science inputs, supported the ISS operations, and revised the manuscript. C. B. developed the experiment hardware and supported the ISS operations.

**Funding** This research is co-sponsored by the National Science Foundation (NSF) and Center for the Advancement of Science in Space (CASIS) under grant number CBET-1740478.

**Data Availability** Data obtained from the ISS experiments will be

made available on NASA's online database after the paper is published. In the meantime, data will be shared upon requests to the corresponding author.

## Declarations

**Ethical Approval** Not applicable.

**Conflict of Interest** The authors declare that they have no known competing financial interests or personal relationships that could have appeared to influence the work reported in this paper.

**Author Consent** All authors agree to be included in the author list of this manuscript and agree to publish this research.

**Open Access** This article is licensed under a Creative Commons Attribution 4.0 International License, which permits use, sharing, adaptation, distribution and reproduction in any medium or format, as long as you give appropriate credit to the original author(s) and the source, provide a link to the Creative Commons licence, and indicate if changes were made. The images or other third party material in this article are included in the article's Creative Commons licence, unless indicated otherwise in a credit line to the material. If material is not included in the article's Creative Commons licence and your intended use is not permitted by statutory regulation or exceeds the permitted use, you will need to obtain permission directly from the copyright holder. To view a copy of this licence, visit <http://creativecommons.org/licenses/by/4.0/>.

## References

- Bhattacharjee, S., Carmignani, L.: Prediction of flame length in opposed-Flow Flame Spread: Global Similarity Analysis and experiments. *Combust. Sci. Technol.* **194**, 2659–2673 (2022). <https://doi.org/10.1080/00102202.2021.1885030>
- Bhattacharjee, S., Wakai, K., Takahashi, S.: Predictions of a critical fuel thickness for flame extinction in a quiescent microgravity environment. *Combust. Flame.* **132**, 523–532 (2003). [https://doi.org/10.1016/S0010-2180\(02\)00501-1](https://doi.org/10.1016/S0010-2180(02)00501-1)
- Bhattacharjee, S., Laue, M., Carmignani, L., Ferkul, P., Olson, S.: Opposed-flow flame spread: A comparison of microgravity and normal gravity experiments to establish the thermal regime. *Fire Saf. J.* **79**, 111–118 (2016). <https://doi.org/10.1016/j.firesaf.2015.11.011>
- Bhattacharjee, S., Simsek, A., Miller, F., Olson, S., Ferkul, P.: Radiative, thermal, and kinetic regimes of opposed-flow flame spread: A comparison between experiment and theory. *Proc. Combust. Inst.* **36**, 2963–2969 (2017). <https://doi.org/10.1016/j.proci.2016.06.025>
- Carmignani, L., Dong, K., Bhattacharjee, S.: Radiation from flames in a Microgravity Environment: Experimental and Numerical investigations. *Fire Technol.* **56**, 33–47 (2020). <https://doi.org/10.1007/s10694-019-00884-y>
- Carney, A., Li, Y., Liao, Y.-T., Olson, S., Ferkul, P.: Concurrent-flow flame spread over thin discrete fuels in microgravity. *Combust. Flame.* **226**, 211–221 (2021). <https://doi.org/10.1016/j.combustflame.2020.12.005>
- Comas, B., Carmona, A., Pujol, T.: Experimental study of the channel effect on the flame spread over thin solid fuels. *Fire Saf. J.* **71**, 162–173 (2015). <https://doi.org/10.1016/j.firesaf.2014.12.001>
- Consalvi, J.-L., Guibaud, A., Coimbra, A., Citerne, J.-M., Legros, G.: Effects of oxygen depletion on soot production, emission and radiative heat transfer in opposed-flow flame spreading over insulated wire in microgravity. *Combust. Flame.* **230**, 111447 (2021). <https://doi.org/10.1016/j.combustflame.2021.111447>
- Cui, W., Sharma, A., Liao, Y.-T.T.: Upward flame spread over discrete thin solids separated by heat-absorbing inert materials. *J. Fire Sci.* **41**, 32–50 (2023). <https://doi.org/10.1177/07349041231153145>
- Feier, I.L., Shih, H.-Y., Sacksteder, K.R., Tien, J.S.: Upward flame spread over thin solids in partial gravity. *Proc. Combust. Inst.* **29**, 2569–2577 (2002). [https://doi.org/10.1016/S1540-7489\(02\)80313-3](https://doi.org/10.1016/S1540-7489(02)80313-3)
- Ferkul, P.V., Olson, S.L., Johnston, M.C., T'ien, J.S.: Flammability aspects of fabric in opposed and concurrent air flow in microgravity. In: 8th US National Combustion Meeting Organized by the Western States Section of the Combustion Institute and hosted by the University of Utah May. pp. 19–22 (2013)
- Guibaud, A., Consalvi, J.-L., Citerne, J.-M., Legros, G.: Pressure effects on the soot production and radiative heat transfer of non-buoyant laminar diffusion flames spreading in opposed flow over insulated wires. *Combust. Flame.* **222**, 383–391 (2020). <https://doi.org/10.1016/j.combustflame.2020.09.003>
- Hossain, S., Wichman, I.S., Sidebotham, G.W., Olson, S.L., Miller, F.J.: Influence of gap height and flow field on global stoichiometry and heat losses during opposed flow flame spread over thin fuels in simulated microgravity. *Combust. Flame.* **193**, 133–144 (2018). <https://doi.org/10.1016/j.combustflame.2018.02.023>
- Hossain, S., Wichman, I.S., Miller, F.J., Olson, S.L.: Opposed flow flame spread over thermally thick solid fuels: Buoyant flow suppression, stretch rate theory, and the regressive burning regime. *Combust. Flame.* **219**, 57–69 (2020). <https://doi.org/10.1016/j.combustflame.2020.05.001>
- Huang, X., Gao, J.: A review of near-limit opposed fire spread. *Fire Saf. J.* **120**, 103141 (2021). <https://doi.org/10.1016/j.firesaf.2020.103141>
- Huang, X., Link, S., Rodriguez, A., Thomsen, M., Olson, S., Ferkul, P., Fernandez-Pello, C.: Transition from opposed flame spread to fuel regression and blow off: Effect of flow, atmosphere, and microgravity. *Proc. Combust. Inst.* **37**, 4117–4126 (2019). <https://doi.org/10.1016/j.proci.2018.06.022>
- Kashiwagi, T., McGrattan, K.B., Olson, S.L., Fujita, O., Kikuchi, M., Ito, K.: Effects of slow wind on localized radiative ignition and transition to flame spread in microgravity. *Symp. Int. Combust.* **26**, 1345–1352 (1996). [https://doi.org/10.1016/S0082-0784\(96\)80353-5](https://doi.org/10.1016/S0082-0784(96)80353-5)
- Kleinhenz, J., Feier, I.L., Hsu, S.-Y., T'ien, J.S., Ferkul, P.V., Sacksteder, K.R.: Pressure modeling of upward flame spread and burning rates over solids in partial gravity. *Combust. Flame.* **154**, 637–643 (2008). <https://doi.org/10.1016/j.combustflame.2008.05.023>
- Konno, Y., Kobayashi, Y., Fernandez-Pello, C., Hashimoto, N., Nakaya, S., Tsue, M., Fujita, O.: Opposed-Flow Flame spread and extinction in Electric wires: The effects of gravity, External Radiant Heat Flux, and wire characteristics on Wire Flammability. *Fire Technol.* **56**, 131–148 (2020). <https://doi.org/10.1007/s10694-019-00935-4>
- Konno, Y., Li, Y., Citerne, J.-M., Legros, G., Guibaud, A., Hashimoto, N., Fujita, O.: Experimental study on downward/opposed flame spread and extinction over electric wires in partial gravity environments. *Proc. Combust. Inst.* (2022). <https://doi.org/10.1016/j.proci.2022.07.002>
- Li, C., Liao, Y.-T.T., T'ien, J.S., Urban, D.L., Ferkul, P., Olson, S., Ruff, G.A., Easton, J.: Transient flame growth and spread processes over a large solid fabric in concurrent low-speed flows in microgravity – model versus experiment. *Proc. Combust. Inst.* **37**, 4163–4171 (2019). <https://doi.org/10.1016/j.proci.2018.05.168>
- Li, Y., Liao, Y.-T.T.: Numerical study of flame spread in a narrow flow duct in microgravity – effects of flow confinement and radiation reflection. *Combust. Flame.* **235**, 111714 (2022). <https://doi.org/10.1016/j.combustflame.2021.111714>

- Li, Y., Liao, Y.-T.T., Ferkul, P.V., Johnston, M.C., Bunnell, C.: Experimental study of concurrent-flow flame spread over thin solids in confined space in microgravity. *Combust. Flame*. **227**, 39–51 (2021a). <https://doi.org/10.1016/j.combustflame.2020.12.042> (a)
- Li, Y., Liao, Y.-T.T., Ferkul, P.V., Johnston, M.C., Bunnell, C.: Confined combustion of polymeric solid materials in microgravity. *Combust. Flame*. **234**, 111637 (2021). <https://doi.org/10.1016/j.combustflame.2021.111637> (b)
- Matsuoka, T., Nakashima, K., Yamazaki, T., Nakamura, Y.: Geometrical effects of a narrow Channel on Flame Spread in an opposed Flow. *Combust. Sci. Technol.* **190**, 409–424 (2018). <https://doi.org/10.1080/00102202.2017.1394848>
- Nagachi, M., Citerne, J.-M., Dutilleul, H., Guibaud, A., Jomaas, G., Legros, G., Hashimoto, N., Fujita, O.: Effect of ambient pressure on the extinction limit for opposed flame spread over an electrical wire in microgravity. *Proc. Combust. Inst.* **38**, 4767–4774 (2021). <https://doi.org/10.1016/j.proci.2020.05.005>
- Olson, S.L.: Mechanisms of Microgravity Flame Spread over a thin solid fuel: Oxygen and opposed Flow effects. *Combust. Sci. Technol.* **76**, 233–249 (1991). <https://doi.org/10.1080/00102209108951711>
- Olson, S.L., Miller, F.J.: Experimental comparison of opposed and concurrent flame spread in a forced convective microgravity environment. *Proc. Combust. Inst.* **32**, 2445–2452 (2009). <https://doi.org/10.1016/j.proci.2008.05.081>
- Olson, S.L., Ferkul, P.V., T'ien, J.S.: Near-limit flame spread over a thin solid fuel in microgravity. *Symp. Int. Combust.* **22**, 1213–1222 (1989). [https://doi.org/10.1016/S0082-0784\(89\)80132-8](https://doi.org/10.1016/S0082-0784(89)80132-8)
- Olson, S.L., Kashiwagi, T., Fujita, O., Kikuchi, M., Ito, K.: Experimental observations of spot radiative ignition and subsequent three-dimensional flame spread over thin cellulose fuels. *Combust. Flame*. **125**, 852–864 (2001). [https://doi.org/10.1016/S0010-2180\(00\)00249-2](https://doi.org/10.1016/S0010-2180(00)00249-2)
- Olson, S.L., Miller, F.J., Jahangirian, S., Wichman, I.S.: Flame spread over thin fuels in actual and simulated microgravity conditions. *Combust. Flame*. **156**, 1214–1226 (2009). <https://doi.org/10.1016/j.combustflame.2009.01.015>
- Olson, S.L., Ferkul, P.V., Bhattacharjee, S., Miller, F.J., Fernandez-Pello, C., Link, S., T'ien, J.S., Wichman, I.: Burning and Suppression of Solids-II (BASS-II) Summary Report. San Diego. (2021)
- Sacksteder, K.R., Greenberg, P.S., Pettegrew, R.D., Tien, J.S., Ferkul, P.V., Shih, H.-Y.: Forced Flow Flame Spreading Test: Preliminary Findings From the USMP-3 Shuttle Mission. Presented at the November 1 (1998)
- Sharma, A., Mishra, K.B.: Experimental investigations on the influence of 'chimney-effect' on fire response of rainscreen façades in high-rise buildings. *J. Build. Eng.* **44**, 103257 (2021). <https://doi.org/10.1016/j.jobbe.2021.103257>
- Takahashi, S., Kondou, M., Wakai, K., Bhattacharjee, S.: Effect of radiation loss on flame spread over a thin PMMA sheet in microgravity. *Proc. Combust. Inst.* **29**, 2579–2586 (2002). [https://doi.org/10.1016/S1540-7489\(02\)80314-5](https://doi.org/10.1016/S1540-7489(02)80314-5)
- Takahashi, S., Ebisawa, T., Bhattacharjee, S., Ihara, T.: Simplified model for predicting difference between flammability limits of a thin material in normal gravity and microgravity environments. *Proc. Combust. Inst.* **35**, 2535–2543 (2015). <https://doi.org/10.1016/j.proci.2014.07.017>
- Urban, D.L., Ferkul, P., Olson, S., Ruff, G.A., Easton, J., T'ien, J.S., Liao, Y.-T.T., Li, C., Fernandez-Pello, C., Torero, J.L., Legros, G., Eigenbrod, C., Smirnov, N., Fujita, O., Rouvreau, S., Toth, B., Jomaas, G.: Flame spread: Effects of microgravity and scale. *Combust. Flame*. **199**, 168–182 (2019). <https://doi.org/10.1016/j.combustflame.2018.10.012>
- Vetturini, A., Cui, W., Liao, Y.-T., Olson, S., Ferkul, P.: Flame spread over ultra-thin solids: Effect of Area Density and concurrent-opposed spread reversal phenomenon. *Fire Technol.* **56**, 91–111 (2020). <https://doi.org/10.1007/s10694-019-00878-w>
- Wang, S., Hu, J., Xiao, Y., Ren, T., Zhu, F.: Opposed-flow Flame Spread over Solid fuels in Microgravity: The Effect of Confined spaces. *Microgravity Sci. Technol.* **27**, 329–336 (2015). <https://doi.org/10.1007/s12217-015-9419-z>
- Zhang, X., Yu, Y.: Experimental studies on the three-dimensional effects of opposed-flow flame spread over thin solid materials. *Combust. Flame*. **158**, 1193–1200 (2011). <https://doi.org/10.1016/j.combustflame.2010.10.004>
- Zhao, X., Liao, Y.-T.T., Johnston, M.C., T'ien, J.S., Ferkul, P.V., Olson, S.L.: Concurrent flame growth, spread, and quenching over composite fabric samples in low speed purely forced flow in microgravity. *Proc. Combust. Inst.* **36**, 2971–2978 (2017). <https://doi.org/10.1016/j.proci.2016.06.028>
- Zhu, F., Huang, X., Wang, S.: Flame Spread over Polyethylene Film: Effects of gravity and fuel inclination. *Microgravity Sci. Technol.* **34**, 26 (2022). <https://doi.org/10.1007/s12217-022-09945-4>

**Publisher's Note** Springer Nature remains neutral with regard to jurisdictional claims in published maps and institutional affiliations.